

Frequency Biases in Pulsed Atomic Fountain Frequency Standards Due to Spurious Components in the Microwave Spectrum

T.P. Heavner, J.H. Shirley, F. Levi[†], D. Yu[‡], S.R. Jefferts

Time and Frequency Division

National Institute of Standards and Technology (NIST)

Boulder, Colorado, U.S.A.

[†]Istituto Nazionale di Ricerca Metrologica (INRIM)
Torino, Italy

[‡]Division of Physical Metrology
Korea Research Institute of Standards and Science (KRISS)
Daejeon, Korea

Abstract—A mechanism by which spurs in the microwave spectrum may cause biases in pulsed atomic fountain frequency standards was identified in [1]. Here we present models for the cases of phase modulating (PM) and amplitude modulating (AM) spurs in the spectrum. In the case of a PM spur, the bias is first-order in the spur amplitude. Under common experimental conditions, this effect may be much larger than the second-order bias presented in [2]. We present measurements made using NIST-F1 whereby PM spurs of known amplitude were added onto the microwave signal used to interrogate the cesium (Cs) clock transition. The measured biases are compared to the predictions of the model. Finally, we discuss the difficulties of evaluating the frequency bias in fountain frequency standards using traditional techniques such as operating at elevated microwave powers.

I. INTRODUCTION

As part of our work aimed at understanding the accuracy of NIST-F1, a laser-cooled cesium (Cs) fountain primary frequency standard at NIST, we have investigated the effect of spurious components in the microwave spectrum (spurs) used to drive the 9.193 GHz clock transition [1]. The starting point for this study is the work by Audoin *et al.* [2], which concerns the case of spurs in Cs thermal beam frequency standards. However, there is a fundamental difference between thermal beams and fountains that makes the result of the analysis of [1], [2] not always applicable. Most Cs fountains operate by use of a periodic, repeating measurement sequence. For example, in NIST-F1 the optical molasses is turned on, cold Cs atoms from the molasses are launched upwards into a state-selection cavity, and undergo Ramsey interrogation, and finally the

populations of the two hyperfine states are determined in the detection zone. This process is repeated many times. Two of these sequences are required to make one frequency measurement using a square-wave line center servo.

In the case of NIST-F1, this measurement sequence is controlled by digital timing electronics with microsecond resolution. Since the Ramsey spectroscopy occurs at the same time during this sequence and it repeats many times ($\approx 10^6$ cycles), spurs in the microwave signal that are synchronous with this sequence may cause a bias. The size of the bias depends strongly on the phase and frequency of the spur with respect to the fountain operation sequence. In a thermal beam standard this effect tends to vanish, since the atoms sample all phases of the spur and the time average of the bias is zero. What remains is the second-order effect described in [2].

It is important to note that although this bias is due to the aliasing of an unwanted spectral component and thus sounds similar to the well known Dick effect [3], it is in fact a different phenomenon. The Dick effect causes degradation in stability due to local oscillator noise in conjunction with dead time in the atomic standard. The effect examined here results in a frequency bias and exists in the absence of dead time.

The theory and measurements presented here show the bias can be quite large, many orders of magnitude larger than the second-order effect described by Audoin *et al.* [2], and depends strongly on the frequency and phase of the spur as well as on the period of the Cs fountain sequence.

Publication of NIST, an agency of the U.S. government; not subject to copyright.

II. THEORY

A. Phase Modulation

In this case, the spur in the microwave signal is considered to modulate the phase of the carrier. We write the field within the Ramsey cavity as proportional to

$$2b_0 \left[\cos \left(\omega_0 t + \frac{b_1}{b_0} \sin(\Delta t + \phi) \right) \right], \quad (0.1)$$

where $2b_0$ is the Rabi frequency of the main part of the field, b_1/b_0 is the amplitude of the phase modulation, Δ is the angular detuning of the spur from the atomic resonance, ω_0 , and ϕ is the phase of the spur when the atom first enters the Ramsey cavity. Although this expression represents balanced upper and lower sidebands with amplitude b_1 , the results presented below are also valid for a single sideband spur with amplitude $2b_1$. We assume (typical for a cold Cs fountain) that the Rabi time of excitation, τ , is much less than the Ramsey time T_R between excitations. Furthermore, we assume that the spur is both small with respect to the carrier, $b_1/b_0 \ll 1$, as well as far from saturation, even when the power in the carrier is elevated; that is, $b_1\tau$ is always much less than 1.

To see why PM can introduce a bias, consider the modulation as a source of a so-called end-to-end phase shift. If the atoms pass through the first excitation region at time t_1 and the second at time $t_2 = t_1 + T_R$, the phase difference due to the modulation will be

$$\delta\Phi = \frac{b_1}{b_0} [\sin(\Delta t_2 + \phi) - \sin(\Delta t_1 + \phi)].$$

Such a phase change causes a frequency shift $\delta\Phi/T_R$. With the aid of a trigonometric identity the resulting frequency bias can be written

$$\frac{\delta\omega}{\omega_0} = \frac{2b_1}{\omega_0 T_R b_0} \sin\left(\frac{1}{2}\Delta T_R\right) \cos\left(\frac{1}{2}\Delta T_R + \phi\right).$$

This formula displays the sinusoidal dependence on initial phase and the Ramsey oscillations with spur detuning. Note that this derivation ignores phase changes during excitation, hence is valid only when $\Delta\tau$ is small.

A more detailed derivation valid for arbitrary spur detuning gives the following result:

$$\frac{\delta\omega}{\omega_0} \approx \frac{4b_1}{T_R \omega_0 \sin 2b_0 \tau} \left[\frac{2b_0 \sin\left(\frac{1}{2}\Delta T_R\right) \sin(2b_0 \tau) - \Delta \cos\left(\frac{1}{2}\Delta T_R\right) \cos(2b_0 \tau)}{\Delta \cos\left(\frac{1}{2}\Delta T_R + \Delta\tau\right)} \right] \frac{\cos\left(\frac{1}{2}\Delta T_R + \Delta\tau + \phi\right)}{4b_0^2 - \Delta^2} \quad (0.2)$$

This result is first-order in the amplitude of the spur. In our derivation the excitation pulses were assumed to have a square profile rather than a half-sine. Finally, the derivation is for a single atom, or equivalently a cloud with a mono velocity distribution. The results here will be slightly modified if averaged over a cold atom velocity distribution. In the case of thermal beams, the phase of the spur, ϕ , evolves over time, and the bias above has a factor given by

$$\langle \cos\left(\frac{1}{2}\Delta T_R + \Delta\tau + \phi\right) \rangle, \quad (0.3)$$

which tends toward zero. Also, a thermal beam has a larger range of Ramsey times, T_R , which, if sufficiently wide, will also make this term average to zero.

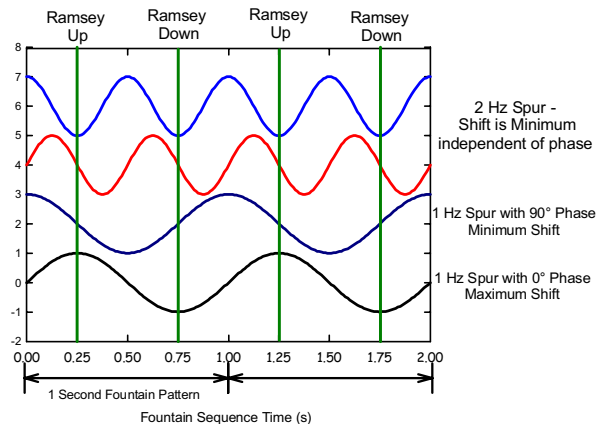


Fig.1. The mechanism by which synchronous spurs may cause frequency biases is graphically illustrated above. The x-axis shows the time evolution of two 1 s sequences of fountain operation. The lowest sinusoidal curve represents the phase evolution of a 1 Hz spur and 0° phase with respect to the fountain sequence. As indicated on the plot, the phase deviation as seen by the atoms is at an extremum at each Ramsey interrogation zone. This additional phase accumulation during each measurement sequence results in a frequency bias. If the phase of the 1 Hz spur is shifted by 90° as illustrated in the next to lowest curve, then the phase deviation as seen by the atoms is the same at each Ramsey interrogation. Hence, there is no bias due to the spur. The upper two plots show the effect when the spur frequency is 2 Hz. Here, the phase deviation as seen by the atoms is always the same at both Ramsey zones, independent of the phase of the spur.

The results of Eq. (0.2), can be explained qualitatively as follows. First, consider the plot shown in Fig. 1. The x-axis shows the time evolution of two 1 s sequences of fountain operation. The lowest sinusoidal curve represents the phase evolution of a 1 Hz spur and 0° phase with respect to the fountain sequence. As indicated on the plot, the phase deviation as seen by the atoms is at an extremum at each Ramsey interrogation zone. This additional phase accumulation during each measurement sequence results in a frequency bias. If the phase of the 1 Hz spur is shifted by 90°, as illustrated in Fig. 1, then the phase deviation as seen by the atoms is the same at each Ramsey interrogation.

Hence, there is no bias due to the spur. The upper two plots in Fig.1 show the effect when the spur frequency is 2 Hz. Here, the phase deviation as seen by the atoms is always the same at both Ramsey zones, independent of the phase of the spur. With the aid of Fig. 1 we begin to see the complex behavior with respect to the frequency and phase of the spur.

B. Amplitude Modulation

Frequency biases can also occur from coherent amplitude modulation (AM). In this case the field within the microwave cavity can be written as

$$2b_0 \left[1 + \frac{b_1}{b_0} \sin(\Delta t + \phi) \right] \cos(\omega_0 t), \quad (0.4)$$

where the variables have the same meanings as previously. In this case, the modulation does not cause a distortion of the Ramsey fringe in first order. However the demodulation process, whether square wave frequency modulation (SQFM) or square wave phase modulation (SQPM) is used, introduces a frequency bias if it is synchronous with the modulation. The order of the bias depends on b_0 , vanishing at optimum power. This is perhaps most easily seen in the case of SQFM. Consider the case where the amplitude modulation executes one cycle every two fountain cycles and where the phase is chosen such that the average amplitude of the microwave field within the cavity on the left side of the Ramsey resonance is a maximum. The average field on the right side of the resonance will then be a minimum. The transition probability on the left side of the line, P_L , will therefore be larger than on the right side of the line, P_R , (assuming that b_0 is set slightly below optimum; the opposite is true if b_0 is slightly above optimum). This introduces a frequency shift

$$\begin{aligned} \frac{\delta\omega}{\omega_0} &\approx \frac{P_L - P_R}{\omega_0 T_R |\sin^2(2b_0\tau)|} \\ &= \frac{(\sin(2b_0\tau) + 2b_1\tau \cos(2b_0\tau))^2 - (\sin(2b_0\tau) - 2b_1\tau \cos(2b_0\tau))^2}{2\omega_0 T_R \sin^2(2b_0\tau)}. \end{aligned} \quad (0.5)$$

Here we have assumed optimum amplitude modulation. Given that the microwave power is not exactly optimum, that is, $2b_0\tau = \pi/2 \pm \epsilon$, then Eq.(0.5) reduces to

$$\frac{\delta\omega}{\omega} \approx \frac{\pi}{\omega_0 T_R} \frac{b_1}{b_0} \epsilon. \quad (0.6)$$

For the simplified case discussed here, if we assume that the AM is -40 dBc, $b_1/b_0 = 1/100$, $T_R = 0.5$ s, and $\epsilon = 0.01$, this leads to a significant frequency bias of $\frac{\delta\omega}{\omega} \approx 5 \times 10^{-15}$.

III. MEASUREMENTS

To test the predictions of the PM spur model, we made several modifications to NIST-F1 that are illustrated in Fig. 2 (at this time, we have not measured the synchronous AM spur model). First, the microwave synthesizer was modified such that the DDS (DDS1 in Fig.2) used to make small frequency corrections to keep lock onto the atomic transition had a small amount of phase modulation. The frequency and phase of the phase modulation was controlled by another DDS (DDS2). Also, the fountain sequence period was adjusted to be $1 \text{ s} \pm 1 \text{ ns}$ in duration. Since the digital electronics controlling the fountain timing were running off the same clock as the frequency generators, this ensured that the spur frequency was synchronous. Defining the phase of the spur is not as trivial since it randomized whenever the frequency of the spur was changed using DDS2. However, Eq. 1.2 provides a recipe for solving this problem. The size of the bias depends on the cosine of the phase of the spur. Then at any given spur frequency, the size of the bias will oscillate about zero. Therefore, once proper experimental conditions are set on the DDS2, the maximum bias can be inferred by measuring the bias at any two phases separated by 90° and adding the results in quadrature. To verify this prediction of the theory, we measured the bias at a fixed spur frequency and varied the phase on DDS2 from 0° to 360° , thus mapping out a sinusoidal curve. The results are shown in

Fig. 3.

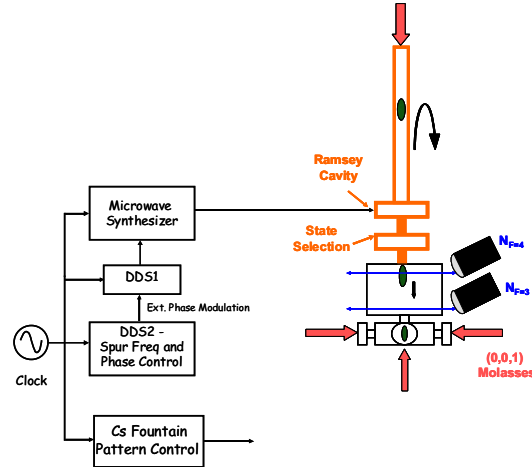


Fig.2. A block diagram of the system used to introduce synchronous spurs into the Cs fountain frequency standard NIST-F1. DDS1, normally used to provide small frequency corrections for the line center servo, was phase modulated. The frequency and phase of the modulation was provided by DDS2. All the synthesizers as well as the digital timing module that controls the fountain measurement sequence operated from the same clock thus ensuring synchronization.

Figure 4 is a plot of the measured maximum bias at a range of frequencies using the method above. The experimental data are shown as points and the solid curve is the prediction of our theory. Clearly, the agreement is very good. For comparison, the second-order bias due to a single sideband presented in [2] is also plotted and is several orders of magnitude smaller. The second-order bias vanishes for

pure modulation.

phase tests.

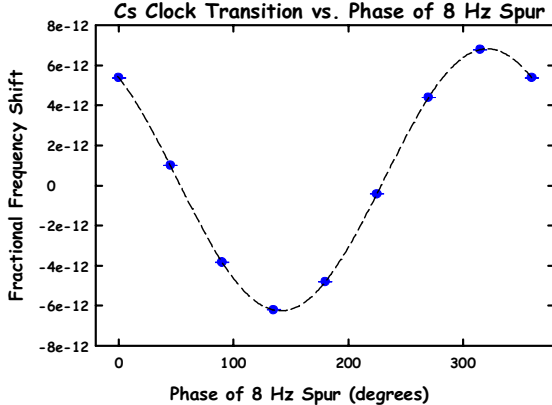


Fig. 3. The measured frequency bias (points) versus the phase of an 8 Hz spur applied to the microwave signal in NIST-F1. The sinusoidal behavior of the bias is predicted by our model presented here. The dashed line is a fit to a sine wave.

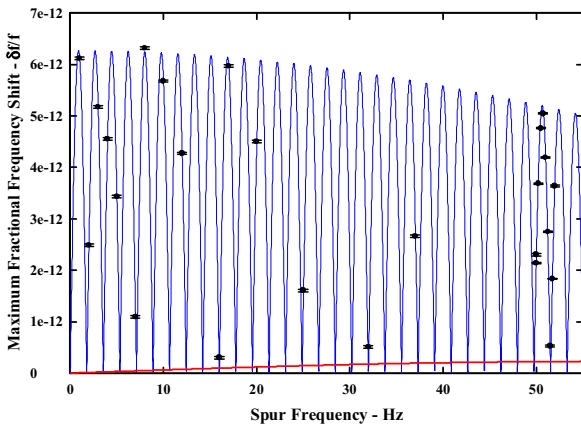


Fig.4. The measured maximum frequency bias versus the spur frequency. The points are measured data and the solid blue curve is the prediction of our model presented here. The red line is the second-order bias predicted by the model from ref [2].

Although we did not measure the power dependence, Fig. 5 presents the power dependence at various spur frequencies as predicted by our model. The power dependence is complex and changes dramatically with small changes in power as well as frequency of the spur. This illustrates the difficulty in extracting meaningful results from power-dependent

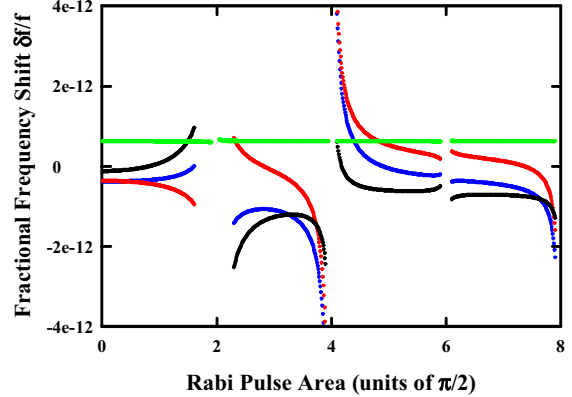


Fig. 5. A plot of the frequency biases due to synchronous spurs at various power levels. The blue curve is for a spur at 60 Hz, the red is 59.5 Hz, black is 60.5 Hz and the green is 1 Hz. This illustrated the difficulty of extracting meaningful conclusions from power sensitivity tests with a synchronous spur in the microwave spectrum.

IV. DISCUSSION

We have developed a model of the frequency bias due to spurs in a pulsed atomic fountain frequency standard and have verified the predictions experimentally using NIST-F1. We conclude that the bias due to such spurs has a complicated dependence upon frequency, phase, and power, and it would be unwise to try to correct for any bias due to spurs. The preferred course of action is to remove or reduce the spurs to a level where they are not a problem. Our work also shows that spurs with balanced sidebands can cause biases.

This frequency bias is not unique to atomic fountains. As with the Dick effect, this bias will appear in any pulsed atomic standard incorporating Ramsey spectroscopy, such as trapped ion and neutral atom standards.

ACKNOWLEDGMENT

The authors thank Archita Hati, Tom Parker, Tom O'Brian, Mike Lombardi, and David Smith for the many helpful comments and suggestions regarding this manuscript.

REFERENCES

- [1] F. Levi, J.H. Shirley, T.P. Heavner, D. Yu, and S.R. Jefferts, "Power dependence of the frequency bias caused by spurious components in the microwave spectrum in atomic fountains," IEEE Trans. Ultrason. Ferr., in press.
- [2] C. Audoin, M. Jardino, L.S. Cutler, R.F. Lacey, "Frequency offset due to spectral impurities in cesium-beam standards," IEEE Trans. Instrum. Meas., vol. IM27, no. 4, pp. 325-329, 1978.
- [3] G.J. Dick, "Local oscillator induced instabilities in trapped ion frequency standards," Proc. 19th Annual PTTI Applications and Planning Meeting, Redondo Beach, CA, 1987, pp. 133-147.